Analytica Chimica Acta 887 (2015) 224–229

Contents lists available at ScienceDirect

Analytica Chimica Acta

journal homepage: www.elsevier.com/locate/aca

# A new signal-on method for the detection of protein based on binding-induced strategy and photoinduced electron transfer between Ag nanoclusters and split G-quadruplex-hemin complexes

Kai Zhang*, Ke Wang, Xue Zhu, Minhao Xie

*Key Laboratory of Nuclear Medicine, Ministry of Health, Jiangsu Key Laboratory of Molecular Nuclear Medicine, Jiangsu Institute of Nuclear Medicine, Wuxi, Jiangsu 214063, China*

## HIGHLIGHTS

- AgNCs have great potential for application in biomedicine.
- Binding of two affinity ligands can result in binding-induced DNA assemblies.
- PET can be happened between DNA/AgNCs and G-quadruplex/hemin complexes.
- A platform for the detection of proteins was proposed by using PET and binding-induced strategy.

## GRAPHICAL ABSTRACT

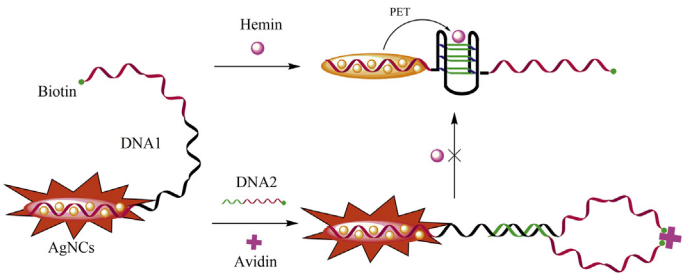


## ARTICLE INFO

*Article history:*
Received 26 June 2015
Received in revised form
28 July 2015
Accepted 31 July 2015
Available online 7 August 2015

*Keywords:*
Ag nanoclusters
G-quadruplex-hemin complexes
Photoinduced electron transfer
Protein detection
Signal-on

## ABSTRACT

Proteins play important roles in biological and cellular processes. The levels of proteins can be useful biomarkers for cellular events or disease diagnosis, thus the method for sensitive and selective detection of proteins is imperative to proteins express, study, and clinical diagnosis. Herein, we report a "signal-on" platform for the assay of protein based on binding-induced strategy and photoinduced electron transfer between Ag nanoclusters and split G-quadruplex-hemin complexes. By using biotin as the affinity ligand, this simple protocol could sensitively detect streptavidin with a detection limit down to 10 pM. With the use of an antibody as the affinity ligand, a method for homogeneous fluorescence detection of Prostate Specific Antigen (PSA) was also proposed with a detection limit of 10 pM. The one-step and wash-free assay showed good selectivity. Its high sensitivity, acceptable accuracy, and satisfactory versatility of analytes led to various applications in bioanalysis.



## 1. Introduction

Few-atom noble nanoclusters, such as gold and silver, are a new class of fluorophores and have great potential for applications in biomedicine [1]. Silver nanoclusters (AgNCs) have been developed as a new class of fluorescent probes since they own an appealing set of features that complements the properties of organic dyes and quantum dots [2]. In addition, AgNCs have desirable photophysical properties and low toxicity suitable for biological applications [3]. In recent years, oligonucleotide-templated silver nanoclusters have attracted special attention due to their facile synthesis, tunable fluorescence emission, and high photostability [4]. Indeed, these new fluorescent materials have been successfully applied in many research fields such as DNA sensing [5,6], small molecule detection

* Corresponding author.
*E-mail address:* zhangkai@jsinm.org (K. Zhang).

http://dx.doi.org/10.1016/j.aca.2015.07.015
0003-2670/

[7], protein assay [1], and cell imaging [8–11]. However, the scarcity of efficient and accurate approaches for modulating the fluorescence of DNA/AgNCs restricts their potential for general application in biomolecules analysis [6,12]. Besides, the use of G-quadruplex/hemin complexes for biosensor design has become an interesting research topic that enables structure-tailoring and function-expanding of well-developed functional DNA molecules toward more versatile applications [13,14]. Enlightened by the above facts, Wang and co-works reported a new proof-of-concept that photo-induced electron transfer (PET) between DNA/AgNCs and G-quadruplex/hemin complexes, accompanied by a decrease in the fluorescence of AgNCs [6]. This strategy was been used to develop a nanocluster-based molecular beacon (NMB) for the detection of DNA and ATP. However, this "signal-off" design was proposed based on the quenching mode, which is not preferred in practice because there were a variety of ligands or solvents that may interfere with PET, leading to "false positive" results. We have also previously developed a PET based sensing platform for the detection of biomolecules. Differently, this strategy allows the architecture to be a "signal-on" biosensor [12]. Nonetheless, it is highly required to develop more methods for the "signal-on" assay of biomolecules since the biosensors built on the "signal-on" routes possess better analytical performance than those on the "signal-off" avenues, which is mainly because of the strong background responses with the "signal-off" biosensors [15].

On the other hand, Le et al.'s recent studies have shown that binding of two affinity ligands to the same target molecule was able to enhance the stability of DNA duplexes by increasing their local concentrations, thus resulting in binding-induced DNA assemblies [16,17]. The increase in local concentrations can be utilized to favor the assembly of DNA sequences that would otherwise be difficult to achieve at low concentrations [18]. This DNA assembly can only be induced by target binding events, which have been used to develop various homogeneous assays for proteins and other molecules. Different with the stability is affected by the concentration of the sequences, the melting temperature (Tm) is usually used to describe the stability of the hybridized complementary sequences [19,20].

Motivated by these previous innovations, we explore here the use of binding-induced DNA association and PET between DNA/AgNCs and G-quadruplex/hemin complexes to propose a new strategy to assay protein concentration. With the use of streptavidin as a proof-of-principle analyte, this sensing platform exhibited high sensitivity and specificity toward streptavidin and prostate specific antigen (PSA) versus other nontargeted proteins.

## 2. Experimental section

### 2.1. Materials and chemicals

All oligonucleotides were purchased from Genscript Biotechnology Co., Ltd (Nanjing, China) and their sequences were as follows: DNA1: 5′-CCT CCT TCC TCC TTG GGT AGG GCG GGT TGG GTT TTT TTT TTT TTT TTT TTT TTT T-Biotin, DNA2: 5′-Biotin-TTT TTT TTT TTT TTT TTT TTT TTT TTT TTC CCA AC-3′, DNA3: 5′-CCT C*T*T TCC TCC TTG GGT AGG GCG GGT TGG GTT TTT TTT TTT TTT TTT TTT TTT T-Biotin, DNA4: 5′-Biotin-TTT TTT TTT TTT TTT TTT TTT TTT TTT TTT TTC *TT*A AC. The underlined letters of DNA3 and DNA4 symbolize the mutant from DNA1 and DNA2, respectively. The stock solutions of DNA were prepared in 20 mM phosphate buffer. Silver nitrate ($AgNO_3$), sodium borohydride ($NaBH_4$), streptavidin, prostate specific antigen (PSA), thrombin, biotin, bovine serum albumin (BSA), alpha fetoprotein (AFP), carcinoembryonic antigen (CEA) and hemin were purchased from Sigma–Aldrich (St. Louis, MO, USA). The stock solution of hemin (5 μM) was prepared in dimethyl sulfoxide (DMSO), stored in darkness at −20 °C. Other chemicals were of reagent grade and were used without further purification. Solutions were prepared with ultrapure water, which was purified with Milli-Q purification system (Branstead) to a specific resistivity of >18.2 MΩ cm).

### 2.2. Fluorescent streptavidin assays

In streptavidin assay, DNA1, DNA2 (1.0 μM each) and varying concentrations of the target protein in 20 mM phosphate buffer (5.0 mM $Mg(Ac)_2$, pH 7.4) was heated at 40 °C for 30 min and then 25 °C for 1 h. A 6 μM solution of $AgNO_3$ was added to the above solution. After 1.0 h at room temperature, 6 μM $NaBH_4$ was added into the mixture. After 14.0 h reaction in the dark, 1.0 μM hemin and 50 mM $KNO_3$ were added, and the mixture was incubated for another 2.0 h, then the fluorescence intensity was measured.

### 2.3. Analysis of prostate specific antigen

To prepare probes for analysis of prostate specific antigen (PSA), DNA1 and DNA2 was first carried out by incubation of 100 μL of 1 μM DNA1 and DNA2 with 500 nM streptavidin in 20 mM phosphate buffer (5.0 mM $Mg(Ac)_2$, pH 7.4) at 37 °C for 1 h. The above solution (100 μL) was then added to 100 μL of 100 nM biotinylated polyclonal anti-PSA antibody (R&D Systems) in 20 mM phosphate buffer (5.0 mM $MMg(Ac)_2$, pH 7.4). After incubation at room temperature for another 1 h to form DNA1-antibody and DNA2-antibody, the solution was stored at 4 °C.

In PSA assay, DNA1-antibody, DNA2-antibody (1.0 μM each) and varying concentrations of the target protein in 20 mM phosphate buffer (5.0 mM $Mg(Ac)_2$, pH 7.4) was heated at 40 °C for 30 min and then 25 °C for 1 h. A 6 μM solution of $AgNO_3$ was added to the above solution. After 1.0 h at room temperature, 6 μM $NaBH_4$ was added into the mixture. After 14.0 h reaction in the dark, 1.0 μM hemin and 50 mM $KNO_3$ were added, and the mixture was incubated for another 2.0 h, and then the fluorescence intensity was measured.

## 3. Results and discussion

### 3.1. The working principle of streptavidin assay

The analysis of streptavidin by the binding-induced aided PET system is depicted schematically in Scheme 1. The system mainly consists of DNA1 and DNA2. DNA1 includes three domains: a sequence that is used to form the DNA/Ag NCs, a sequence that is partly complementary to DNA2 along with the G-quadruplex sequence, and a linker part. DNA2 includes two domains: a sequence that is complementary to DNA1, caging the G-quadruplex sequence of DNA1 into a protected inactive configuration that eliminates the formation of the active G-quadruplex/hemin structure, and a linker part. The design principle is guided by $T_m$ differences between the DNA1-streptavidin-DNA2 complex and the free hybrids of two strands. It is necessary to minimize the hybridization between the two complementary sequences in the absence of the target. Key to the success of this strategy is the binding-induced hybridization which is triggered by the binding of the two strands to the target protein. If streptavidin is present in the assay solution at the beginning, target recognition is achieved by two specific affinity ligands binding to the streptavidin. One affinity ligand is linked to DNA1, which serves as the scaffold for the signal translator. The second affinity ligand is conjugated to DNA2, which serves as the competing DNA. Thus, in the absence of the molecular target, the formation of DNA1-DNA2 duplex is minimal, allowing self-assembly of the G-quadruplex/hemin complex, which results in the quenching of the fluorescence of the DNA/AgNCs. However,

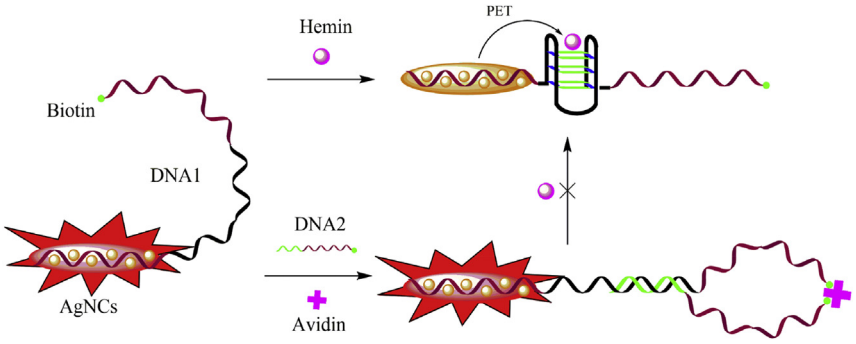


**Scheme 1.** Schematic illustration of the analysis of streptavidin using the PET between DNA/AgNCs-G-quadruplex-hemin complex.

in the presence of the target molecule, the binding of the target molecule to the two affinity ligands that are linked to DNA1 and DNA2 brings DNA2 into close proximity to the DNA1. This binding-induced assembly of DNA2 around the DNA1 greatly increases the local concentration of DNA2. As a consequence, a part of the G-quadruplex sequence forms a stable duplex domain during the formation of DNA1-DNA2 duplex, caging the G-quadruplex sequence into a protected inactive configuration that eliminates the formation of the active G-quadruplex/hemin structure, which leads to the retention of the fluorescence of the DNA/AgNCs.

### 3.2. Feasibility study of the streptavidin assay

The goal is to have much higher $T_m$ for the hybrid in the binding induced assembly DNA1-streptavidin-DNA2 than for the hybrid in DNA1-DNA2 complex, so that DNA1-streptavidin-DNA2 is stable while DNA1-DNA2 duplex is unstable at room temperature. We used OligoAnalyzer 3.1 (free software from IDT) to estimate the $T_m$ of the hybrid in DNA1-DNA2 complex and in the binding-induced assembly DNA1-streptavidin-DNA2. The input parameters used for these estimations were 1 μM DNA, 20 mM $Na^+$, and 5 mM $Mg^{2+}$. To estimate the $T_m$ of the binding-induced assembly DNA1-streptavidin-DNA2, a hairpin structure with a loop containing 100 thymidines was used [16]. The estimated $T_m$ difference between the binding-induced assembly DNA1-streptavidin-DNA2 (38.3 °C) and the DNA1-DNA2 duplex (14 °C) was >24 °C. This large difference in thermal stability enabled successful formation of the binding-induced assembly while diminishing the background due to self-assembly.

In order to test the veracity of the strategy, DNA3 and DNA4, with only one or two nucleotide differences between DNA1 and DNA2, are employed as the control oligonucleotides. Fig. 1 shows the fluorescent emission spectrum of the: DNA-AgNCs obtained using DNA1 as the synthetic scaffold (curve a), DNA3 as the synthetic scaffold (curve b), DNA1/DNA4/hemin/AgNCs treated with 5000 pM streptavidin (curve c), and DNA1-AgNCs/DNA2 treated with hemin (curve d), respectively. From the results presented in Fig. 1, we may conclude that: 1). Compared curve (a) with curve (b), DNA3 may not form DNA-AgNCs as a synthetic scaffold effectively; 2). Compared curve (c) with curve (d), DNA4 may not hybridize with DNA1 effectively, which makes the DNA1 templated "free" in the solution, leading to the formation of the active G-quadruplex/hemin structure, which resulted in an decrease in the fluorescence intensity.

To verify the feasibility of the method, the fluorescence changes that occur during the emission of AgNCs under different conditions were investigated. Fig. 2A shows the emission spectrum of the fluorescent DNA-AgNCs obtained using DNA1 as the synthetic scaffold. The formed DNA1-Ag NCs shows strong fluorescence intensity at 655 nm (curve e). After the introduction of only DNA2 (curve d) or DNA2 and streptavidin (curve c) to DNA1/AgNCs solution, there are almost no change in the fluorescence emission, indicating that the presence of DNA2 or DNA2/streptavidin could not influence the fluorescence intensity. After the introduction of hemin (curve a) to above DNA1/DNA2 system, the fluorescence intensity decreased sharply. This result indicates that the excited electrons of the DNA/AgNCs can be transferred to the G-quadruplex-hemin complex in this strategy and DNA2 cannot influence the formation of G-quadruplex-hemin complex. However, upon addition of 5000 pM streptavidin before the formation of G-quadruplex-hemin complex (curve b), the fluorescence intensity only slightly smaller than that of DNA1/AgNCs fluorescence intensity. This result indicates that the target streptavidin could combine with the recognition part of DNA1 and DNA2 to form the DNA1/DNA2 duplex, caging the G-quadruplex sequence into a protected inactive configuration that eliminates the formation of the active G-quadruplex/hemin structure, which results in an increase in the fluorescence intensity.

### 3.3. Sensitivity and selectivity of the streptavidin sensing system

Fig. 2B shows the fluorescence emission intensity in the presence of different concentrations of target streptavidin. The result shows that as the concentration of streptavidin increased, the fluorescence intensity obviously increased. The result is certainly

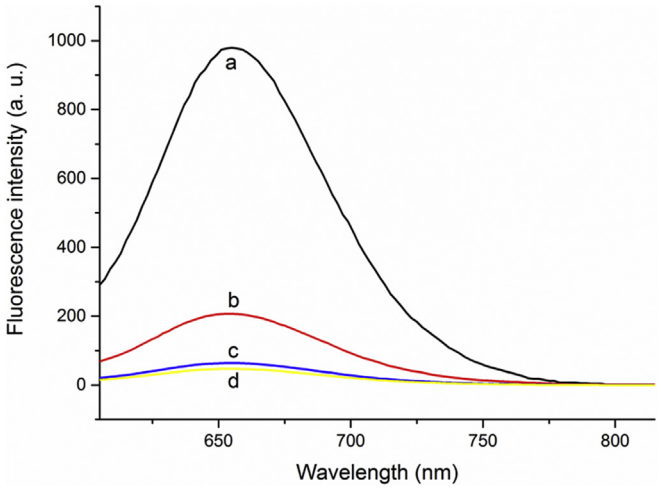


**Fig. 1.** Veracity test. Emission spectra of DNA-AgNCs under different conditions: (a) DNA1/AgNCs; (b) DNA3/AgNCs; (c) DNA1/DNA4/hemin/AgNCs treated with 5000 pM streptavidin; (d) DNA1/DNA2/hemin/AgNCs, respectively.

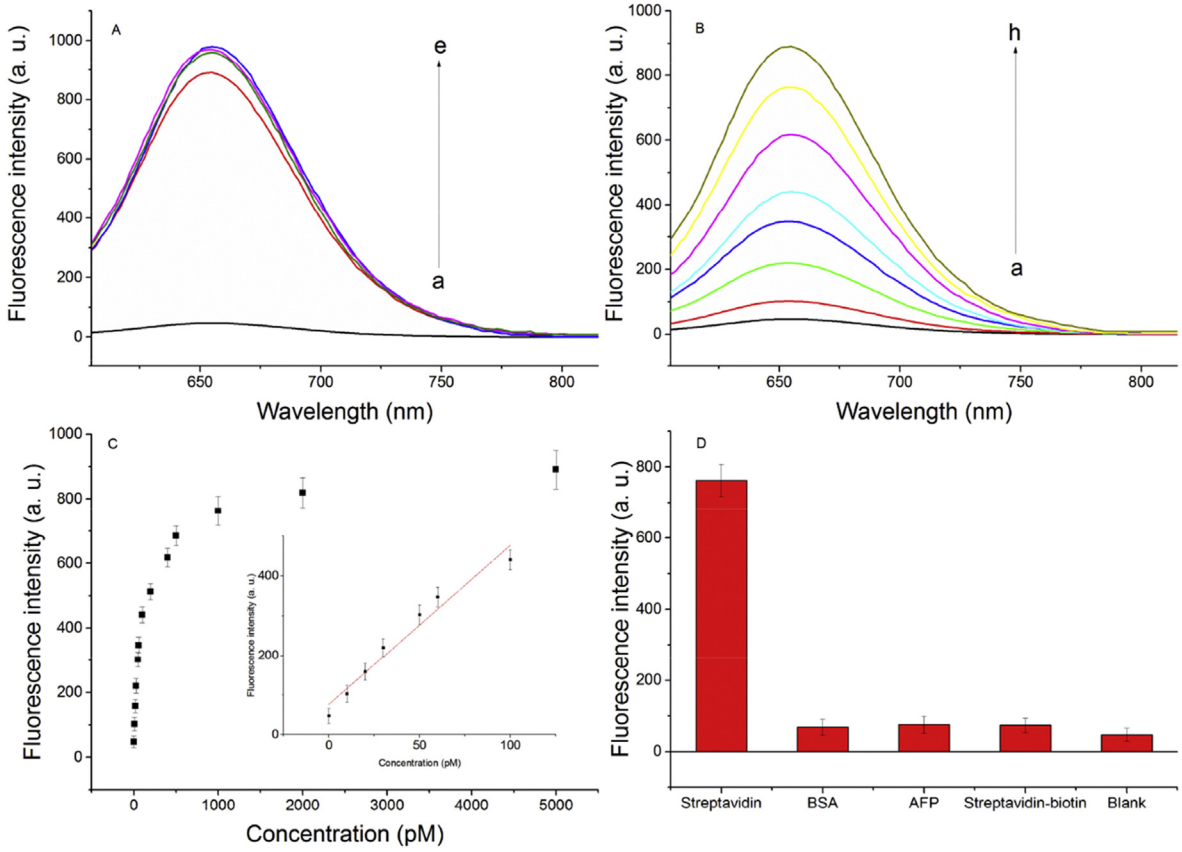


**Fig. 2.** (A) Emission spectra of DNA-AgNCs under different conditions: (a) DNA1/DNA2/hemin/AgNCs; (b) DNA1/DNA2/hemin/AgNCs treated with 5000 pM streptavidin; (c) DNA1/DNA2/AgNCs treated with 5000 pM streptavidin; (d) DNA1/DNA2/AgNCs; and (e) DNA1/AgNCs, respectively. (B) Fluorescence emission spectra at different streptavidin concentrations (0, 10, 30, 60, 100, 400, 1000, and 5000 pM from a to h). (C) Relationship between the fluorescence intensity and the concentration of streptavidin. The inset shows a linear relationship over the concentration from 0 to 100 pM. (D) Selectivity of target streptavidin analysis.

reasonable, because a high concentration of streptavidin will combine a large quantity of DNA1 and DNA2, making more caged G-quadruplex sequence into a protected inactive configuration that eliminates the formation of the active G-quadruplex/hemin structure, which leads to the retention of the fluorescence of the DNA/AgNCs. Fig. 2C presents the relationship between the fluorescence emission intensity and the quantity of streptavidin, and the inset shows the calibration curve for the analysis of streptavidin. A good linear range from 0 to 100 pM with an equation $Y = 4.01\ X+76.34$ ($R^2 = 0.954$), where Y is the fluorescence intensity and X is the concentration of streptavidin, and the detection limit was found to be 10 pM (blank tests plus $3\sigma$, $\sigma$ is the standard deviation of the blank solution, $n > 3$) (Fig. 2C inset). The sensitivity is much better to the previously reported fluorescent dye-based streptavidin detection methods [18]. To test the specificity of this sensing system, streptavidin that was fully saturated with biotin (streptavidin-biotin), BSA, and AFP were investigated. It is found that streptavidin resulted in an obvious change in the fluorescence, while the fluorescence intensities in the presence of bovine serum albumin (BSA), and alpha fetoprotein (AFP), and streptavidin-biotin are similar to that of the blank (Fig. 2D). These results demonstrate that this strategy exhibits excellent selectivity for streptavidin detection.

### 3.4. The working principle of PSA assay

To demonstrate the general applicability of this strategy to ultrasensitive detection of other proteins, a homogeneous model was adopted for the detection of PSA by using antibodies as affinity ligands. As shown in Scheme 2, biotinylated polyclonal antibody for PSA was used to recognize PSA. One biotinylated polyclonal antibody was linked to DNA1 via the streptavidin-biotin bridge, forming DNA1-antibody. Another biotinylated polyclonal antibody was linked to DNA2, forming DNA2-antibody. Binding of the two antibody modified DNA to PSA resulted in the close proximity of DNA1 and DNA2. As a consequence, a part of the G-quadruplex sequence on DNA1 forms a stable duplex domain during the formation of DNA1-DNA2 duplex, caging the G-quadruplex sequence into a protected inactive configuration that eliminates the formation of the active G-quadruplex/hemin structure, which leads to the retention of the fluorescence of the DNA/AgNCs.

### 3.5. Feasibility study of the PSA assay

Similarly, the fluorescence changes were investigated to verify the feasibility (Fig. 3A). The DNA1-antibody/Ag NCs showed strong fluorescence intensity (curve e). The addition of DNA2-antibody (curve d) and DNA2-antibody/PSA (curve c) to DNA1-antibody/AgNCs solution bring no obvious changes of the fluorescence intensity. But, the introduction of hemin (curve a) to above DNA1-antibody/Ag NCs/DNA2-antibody solution, the fluorescence intensity decreased sharply. This result also indicates that the excited electrons of the DNA/AgNCs can be transferred to the G-quadruplex-hemin complex in this method. Identically, upon addition of 5000 pM target PSA before the formation of G-quadruplex-hemin complex (curve b), the fluorescence intensity only slightly smaller than that of DNA-antibody/AgNCs fluorescence intensity.

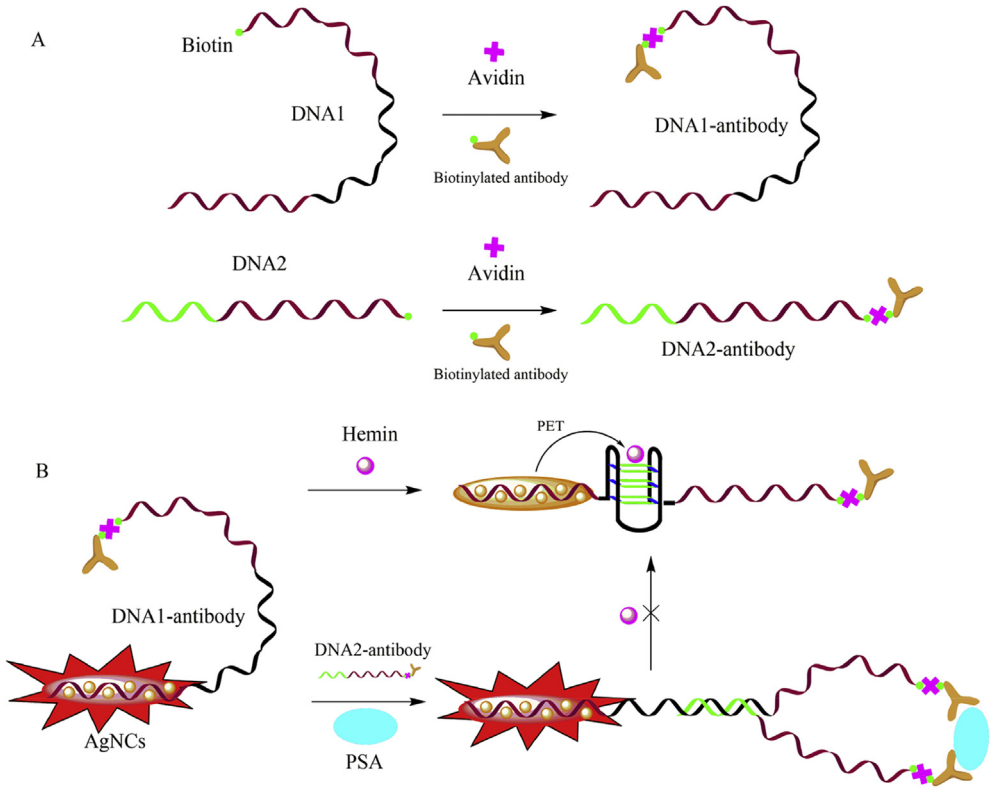


**Scheme 2.** (A) Schematic illustration of the principle of the formation of DNA1-antibody and DNA2-antibody. (B) Schematic illustration of the analysis of PSA using the PET between DNA/AgNCs-G-quadruplex-hemin complex.

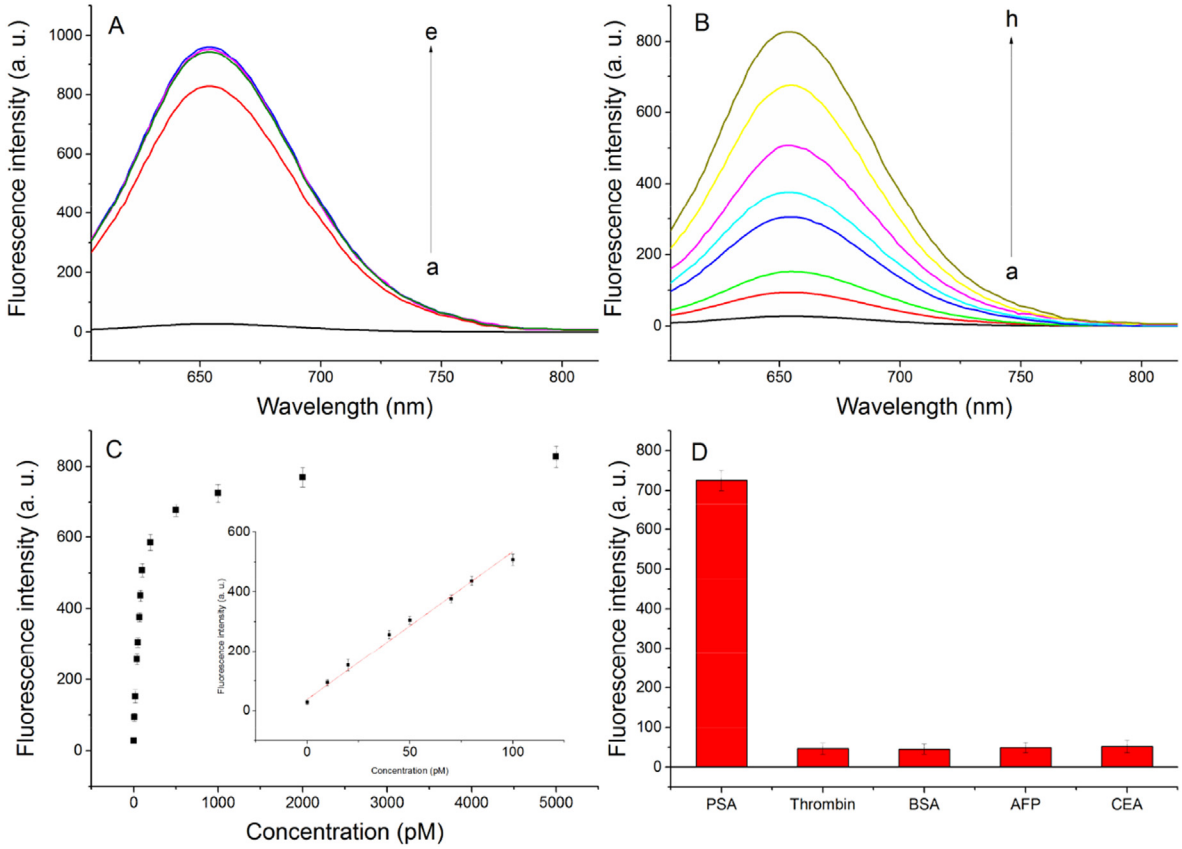


**Fig. 3.** (A) Emission spectra of DNA-AgNCs under different conditions: (a) DNA1-antibody/DNA2-antibody/hemin/AgNCs; (b) DNA1-antibody/DNA2-antibody/hemin/AgNCs treated with 5000 pM PSA; (c) DNA1-antibody/DNA2-antibody/AgNCs treated with 5000 pM PSA; (d) DNA1-antibody/DNA2-antibody/AgNCs; and (e) DNA1-antibody/AgNCs, respectively. (B) Fluorescence emission spectra at different PSA concentrations (0, 10, 20, 50, 70, 100, 500, and 5000 pM from a to h). (C) Relationship between the fluorescence intensity and the concentration of PSA. The inset shows a linear relationship over the concentration from 0 to 100 pM. (D) Selectivity of target PSA analysis.

### 3.6. Sensitivity and selectivity of the PSA sensing system

We further explored the fluorescence emission spectra of the AgNCs-G-quadruplex/hemin interaction in the presence of different concentrations of PSA (Fig. 3B), obviously, the fluorescent signal intensity increased along with the concentration of PSA. This significant signal gain is an inherent advantage of the "signal-on" sensors as compared with the "signal-off" ones. Fig. 3C shows the relationship between the fluorescence intensity and the PSA concentration, and the inset shows the calibration curve for quantitative analysis of PSA. The intensity was linearly dependent on the concentration of PSA over the range from 0 to 100 pM using an equation $Y = 4.97\ X + 39.70$ ($R^2 = 0.992$), where Y is the fluorescence intensity and X is the concentration of PSA, and a detection limit of 10 pM (as ~0.33 ng $mL^{-1}$) could be obtained according to the responses of the blank tests plus 3 times the standard deviation (3σ) (Fig. 3C insert). This is lower than or comparable to the detection limits for most of the previously reported AgNC based biosensors (0.59 ng $mL^{-1}$ [21], 4 ng $mL^{-1}$ [22], and 5 ng $mL^{-1}$ [23]), Enzyme-Linked ImmunoSorbent Assay (ELISA) (1.25 ng $mL^{-1}$ [24]), and nanoprobes based methods (4 ng $mL^{-1}$ [25]) for PSA detection. Similarly, the specificity of this sensing system was also investigated by examining whether other common proteins would interfere with the assay of PSA (Fig. 3D). Four proteins, thrombin, BSA, AFP, and carcinoembryonic antigen (CEA) were chosen to be tested under the same experimental conditions as those for PSA. It was found that PSA resulted in an obvious change in the fluorescence, while the fluorescence changes in the presence of other proteins were nearly negligible. These results demonstrate that this approach exhibits excellent selectivity for PSA detection over other proteins. The good selectivity probably came from the specific antigen–antibody interaction of PSA with polyclonal antibody.

## 4. Conclusions

In summary, we have successfully developed a binding-induced fluorescence turn-on strategy for the detection of protein based on the photoinduced electron transfer between Ag nanoclusters and split G-quadruplex-hemin complexes. Binding of the specific protein to affinity ligands on DNA1 and DNA2 lead to increased local concentrations of them, thereby resulting in binding-induced strand hybridization. The hybridization was forbiddance the formation of G-quadruplex-hemin complexes, which resulted in an increase in the fluorescence intensity. This strategy has been used for the detection of streptavidin and PSA with high sensitivity and selectivity. More importantly, the strategy can also be applied to construct binding induced assay for the molecular targets which can bind to two affinity probes, such as Thrombin, PDGF-BB.

## Acknowledgment

This work is supported by the Social Development Fund of Jiangsu Province (BE2013614), the Grants from National Natural Science Foundation (81300787), the Natural Science Foundation of Jiangsu Province (BK2011168, BK2012105, BK20041103), and Technology Infrastructure Plan of Jiangsu Province-Technology Public Service Platform (BM2012066).

## References

[1] L. Zhang, J. Zhu, Z. Zhou, S. Guo, J. Li, S. Dong, E. Wang, A new approach to light up DNA/Ag nanocluster-based beacons for bioanalysis, Chem. Sci. 4 (2013) 4004–4010.
[2] K. Zhang, K. Wang, X. Zhu, J. Zhang, L. Xu, B. Huang, M. Xie, Label-free and ultrasensitive fluorescence detection of cocaine based on a strategy that utilizes DNA-templated silver nanoclusters and the nicking endonuclease-assisted signal amplification method, Chem. Commun. 50 (2014) 180–182.
[3] Z. Yuan, Y.-C. Chen, H.-W. Li, H.-T. Chang, Fluorescent silver nanoclusters stabilized by DNA scaffolds, Chem. Commun. 50 (2014) 9800–9815.
[4] S. Walczak, K. Morishita, M. Ahmed, J. Liu, Towards understanding of polyguanine activated fluorescent silver nanoclusters, Nanotechnology 25 (2014) 155501–155509.
[5] Y. Tao, Y. Lin, Z. Huang, J. Ren, X. Qu, DNA-templated silver nanoclusters-graphene oxide nanohybrid materials: a platform for label-free and sensitive fluorescence turn-on detection of multiple nucleic acid targets, Analyst 137 (2012) 2588–2592.
[6] L. Zhang, J. Zhu, S. Guo, T. Li, J. Li, E. Wang, Photoinduced Electron Transfer of DNA/Ag Nanoclusters Modulated by G-Quadruplex/Hemin Complex for the Construction of Versatile Biosensors, J. Am. Chem. Soc. 135 (2013) 2403–2406.
[7] M. Zhang, S.-M. Guo, Y.-R. Li, P. Zuo, B.-C. Ye, A label-free fluorescent molecular beacon based on DNA-templated silver nanoclusters for detection of adenosine and adenosine deaminase,, Chem. Commun. 48 (2012) 5488–5490.
[8] Y.W. Zhou, C.M. Li, Y. Liu, C.Z. Huang, Effective detection and cell imaging of prion protein with new prepared targetable yellow-emission silver nanoclusters, Analyst 138 (2013) 873–878.
[9] Y. Tao, Z.H. Li, E.G. Ju, J.S. Ren, X.G. Qu, One-step DNA-programmed growth of CpG conjugated silver nanoclusters: a potential platform for simultaneous enhanced immune response and cell imaging, Chem. Commun. 49 (2013) 6918–6920.
[10] J.J. Li, W.J. Wang, D.F. Sun, J.N. Chen, P.H. Zhang, J.R. Zhang, Q.H. Min, J.J. Zhu, Aptamer-functionalized silver nanoclusters-mediated cell type-specific siRNA delivery and tracking, Chem. Sci. 4 (2013) 3514–3521.
[11] J. Yin, X. He, K. Wang, Z. Qing, X. Wu, H. Shi, X. Yang, One-step engineering of silver nanoclusters-aptamer assemblies as luminescent labels to target tumor cells, Nanoscale 4 (2012) 110–112.
[12] K. Zhang, K. Wang, X. Zhu, Y. Gao, M. Xie, Rational design of signal-on biosensors by using photoinduced electron transfer between Ag nanoclusters and split G-quadruplex halves-hemin complexes, Chem. Commun. 50 (2014) 14221–14224.
[13] Z.-H. Wang, C.-Y. Lu, J. Liu, J.-J. Xu, H.-Y. Chen, An improved G-quadruplex DNAzyme for dual-functional electrochemical biosensing of adenosines and hydrogen peroxide from cancer cells, Chem. Commun. 50 (2014) 1178–1180.
[14] Z. Zhou, Y. Du, L. Zhang, S. Dong, A label-free, G-quadruplex DNAzyme-based fluorescent probe for signal-amplified DNA detection and turn-on assay of endonuclease,, Biosens. Bioelectron. 34 (2012) 100–105.
[15] W.-W. Zhao, J.-J. Xu, H.-Y. Chen, Photoelectrochemical DNA Biosensors, Chem. Rev. 114 (2014) 7421–7441.
[16] H. Zhang, X.-F. Li, X.C. Le, Binding-induced DNA assembly and its application to yoctomole detection of proteins, Anal. Chem. 84 (2011) 877–884.
[17] F. Li, H. Zhang, Z. Wang, X. Li, X.-F. Li, X.C. Le, Dynamic DNA assemblies mediated by binding-induced DNA strand displacement, J. Am. Chem. Soc. 135 (2013) 2443–2446.
[18] F. Li, H. Zhang, C. Lai, X.-F. Li, X.C. Le, A molecular translator that acts by binding-induced DNA strand displacement for a homogeneous protein assay, Angew. Chem. Int. Ed. 51 (2012) 9317–9320.
[19] S. Shen, X.-F. Li, W.R. Cullen, M. Weinfeld, X.C. Le, Arsenic binding to proteins, Chem. Rev. 113 (2013) 7769–7792.
[20] H. Zhang, F. Li, B. Dever, X.-F. Li, X.C. Le, DNA-mediated homogeneous binding assays for nucleic acids and proteins, Chem. Rev. 113 (2012) 2812–2841.
[21] H.D. Jang, S.K. Kim, H. Chang, J.-W. Choi, 3D label-free prostate specific antigen (PSA) immunosensor based on graphene–gold composites, Biosens. Bioelectron. 63 (2015) 546–551.
[22] J. Okuno, K. Maehashi, K. Kerman, Y. Takamura, K. Matsumoto, E. Tamiya, Label-free immunosensor for prostate-specific antigen based on single-walled carbon nanotube array-modified microelectrodes, Biosens. Bioelectron. 22 (2007) 2377–2381.
[23] C. Li, M. Curreli, H. Lin, B. Lei, F.N. Ishikawa, R. Datar, R.J. Cote, M.E. Thompson, C. Zhou, Complementary detection of prostate-specific antigen using In2O3 nanowires and carbon nanotubes, J. Am. Chem. Soc. 127 (2005) 12484–12485.
[24] J. Liang, C. Yao, X. Li, Z. Wu, C. Huang, Q. Fu, C. Lan, D. Cao, Y. Tang, Silver nanoprism etching-based plasmonic ELISA for the high sensitive detection of prostate-specific antigen, Biosens. Bioelectron. 69 (2015) 128–134.
[25] M.-S. Wu, D.-J. Yuan, J.-J. Xu, H.-Y. Chen, Electrochemiluminescence on bipolar electrodes for visual bioanalysis, Chem. Sci. 4 (2013) 1182–1188.